Received: 1 June 2022 | Revised: 26 September 2022 | Accepted: 16 October 2022

DOI: 10.1002/psp4.12880

ARTICLE

Model-based population pharmacokinetic analysis of tislelizumab in patients with advanced tumors

Nageshwar Budha[1] | **Chi-Yuan Wu**[1] | **Zhiyu Tang**[1] | **Tian Yu**[1] | **Lucy Liu**[2] | **Fengyan Xu**[2] | **Yuying Gao**[2] | **Ruiying Li**[3] | **Qiuyang Zhang**[3] | **Ya Wan**[3] | **Srikumar Sahasranaman**[1]

[1]Clinical Pharmacology, BeiGene (USA), Inc., San Mateo, California, USA

[2]Pharmacometrics, Shanghai Qiangshi Information Technology Co., Ltd., Shanghai, China

[3]Clinical Pharmacology, BeiGene (Shanghai), Co., Ltd, Shanghai, China

Correspondence
Srikumar Sahasranaman, Clinical Pharmacology, BeiGene (USA), Inc., 1840 Gateway Drive, San Mateo, CA, USA.
Email: sri.sahasranaman@beigene.com

Abstract

Tislelizumab, a humanized immunoglobulin G4 monoclonal antibody, is a programmed cell death protein 1 (PD-1) inhibitor designed to minimize Fc gamma receptor binding on macrophages to limit antibody-dependent phagocytosis, a potential mechanism of resistance to anti–PD-1 therapy. The pharmacokinetic (PK) profile of tislelizumab was analyzed with population PK modeling using 14,473 observed serum concentration data points from 2596 cancer patients who received intravenous (i.v.) tislelizumab at 0.5–10 mg/kg every 2 weeks or every 3 weeks (q3w), or a 200 mg i.v. flat dose q3w in 12 clinical studies. Tislelizumab exhibited linear PK across the dose range tested. Baseline body weight, albumin, tumor size, tumor type, and presence of antidrug antibodies were identified as significant covariates on central clearance, whereas baseline body weight, sex, and age significantly affected central volume of distribution. Sensitivity analysis showed that these covariates did not have clinically relevant effects on tislelizumab PK. Other covariates evaluated, including race (Asian vs. White), lactate dehydrogenase, estimated glomerular filtration rate, renal function categories, hepatic function measures and categories, Eastern Cooperative Oncology Group performance status, therapy (monotherapy vs. combination therapy), and line of therapy did not show a statistically significant impact on tislelizumab PK. These results support the use of tislelizumab 200 mg i.v. q3w without dose adjustment in a variety of patient subpopulations.

STUDY HIGHLIGHTS

WHAT IS THE CURRENT KNOWLEDGE ON THE TOPIC?

Tislelizumab is an antiprogrammed cell death protein 1 (PD-1) antibody with antitumor activity and a tolerable safety profile in patients with various advanced or metastatic cancers.

WHAT QUESTION DID THIS STUDY ADDRESS?

The analysis characterized tislelizumab pharmacokinetics (PK) and explored the effects of covariates on tislelizumab PK. The feasibility of a flat dose regimen was also assessed in comparison with simulated body weight–based dosing.

WHAT DOES THIS STUDY ADD TO OUR KNOWLEDGE?

The analysis shows that tislelizumab PK is linear across the dose range tested. Tislelizumab exposures are similar across various covariates, including body weight and tumor type, and clinical factors such as hepatic and renal status have no significant effect on tislelizumab PK. These results support the use of tislelizumab 200 mg intravenously every 3 weeks without dose adjustment in a variety of patient subpopulations.

HOW MIGHT THIS CHANGE DRUG DISCOVERY, DEVELOPMENT, AND/OR THERAPEUTICS?

The model supports a flat dosing regimen for tislelizumab across multiple oncologic indications to provide a more practical clinical dose regimen.

INTRODUCTION

The programmed cell death protein 1 (PD-1)/programmed death-ligand 1 (PD-L1) axis plays a central role in suppressing antitumor activity.[1] Binding of PD-1 to PD-L1 on tumor cells downregulates cytotoxic T-cell responses. Blockade of this interaction with PD-1/PD-L1 inhibitor therapy releases T cells from the inhibitory effects of PD-1, thereby inducing an antitumor immune response.[2–4] In recent years, immunotherapy targeting the PD-1/PD-L1 pathway has become an important strategy for cancer treatments, and immune checkpoint inhibitors have demonstrated substantial clinical benefits for cancer patients treated with mono- or combination immunotherapies.[5] However, multiple mechanisms of primary and secondary resistance to PD-1/PD-L1 pathway blockade exist, including antibody clearance (CL) via antibody-dependent cellular phagocytosis (ADCP) through macrophage Fc gamma receptor (FcγR) binding.[6]

Tislelizumab (BGB-A317) is a humanized immunoglobulin (Ig) G4 monoclonal antibody with high affinity and binding specificity for PD-1.[6,7] Tislelizumab was designed to minimize FcγR binding on macrophages to limit ADCP.[6,8] In preclinical studies, binding to FcγR on macrophages has been shown to compromise the antitumor activity of PD-1 antibodies through activation of antibody-dependent, macrophage-mediated killing of T effector cells.[6] Tislelizumab demonstrated high target affinity and a slow dissociation rate from PD-1 and showed a longer binding time, different binding orientation, and more complete blockade of PD-1/PD-L1 interaction compared with pembrolizumab and nivolumab in preclinical models.[9] Tislelizumab is being developed as a monotherapy and in combination with other therapies for the treatment of a broad array of both solid tumors and hematologic cancers.

Tislelizumab has shown robust antitumor activity and was generally well tolerated in patients with advanced tumors,[1,10] which led to conditional approvals in China for previously treated classical Hodgkin lymphoma (cHL),[11] previously treated urothelial carcinoma (UC),[12] and previously treated hepatocellular carcinoma (HCC).[13] Full approvals have been granted in China for advanced squamous and nonsquamous non-small cell lung cancer (NSCLC) in combination with chemotherapy in the first-line setting and as a second- or third-line treatment for patients with locally advanced or metastatic NSCLC.[13–15]

To inform the clinical usage of tislelizumab, it is necessary to better understand its pharmacokinetic (PK) properties across different patient populations and to ensure an appropriate dose is given to these populations. The aim of this analysis was to describe the PK of tislelizumab in patients with cancer and estimate typical values and interpatient variability in PK parameters. The study also aimed to evaluate the effect of patient demographics, pathophysiologic factors, immunogenicity, and organ function on tislelizumab PK to identify the clinical factors that might affect tislelizumab exposure in individual patients. In addition, we aimed to evaluate the impact of body weight (WT) distribution on flat dosing and WT-based dosing regimens for tislelizumab using a population PK (PopPK) simulation approach.

METHODS

Analysis dataset

This analysis was based on data from the following 12 studies, in which patients were treated with tislelizumab in a dose range of 0.5 mg/kg to 10 mg/kg every 2 weeks (q2w) or every 3 weeks (q3w), or 200 mg q3w

administered by intravenous (i.v.) infusion (Table 1): phase Ia/Ib BGB-A317-001; phase I/II BGB-A317-102; phase II BGB-A317-203, BGB-A317-204, BGB-A317-205, BGB-A317-206, BGB-A317-208, BGB-A317-209; phase III BGB-A317-302, BGB-A317-303, BGB-A317-304, and BGB-A317-307. Patients in the analysis had either solid tumors or cHL. All relevant institutional review boards/independent ethics committees reviewed the protocols and amendments and approved the studies, which were carried out in accordance with the International Conference on Harmonisation Good Clinical Practice Guideline, the principles of the Declaration of Helsinki, and local laws and regulations.

Patients were defined as evaluable for PopPK analysis if they had at least one adequately documented tislelizumab administration and a corresponding PK sample collection after the dose. Tislelizumab serum concentrations in the samples were quantified using validated bioanalytical assays using an enzyme-linked immunosorbent assay method. The lower limit of quantification for tislelizumab was 400 ng/ml. The antidrug antibody (ADA) binding assay employed the electrochemiluminescence immunoassay method to detect the presence of anti-tislelizumab antibodies in human serum.

A small percentage of postbaseline concentration data (0.358% [52/14,543]) were below the limit of quantification and were therefore omitted from the PopPK dataset. Suspected data errors were identified by data examination prior to modeling and excluded from the subsequent PopPK analysis. Outliers were primarily evaluated by conditional weighted residual (CWRES) error of the final base model, and observations for which |CWRES| were >5 were considered outliers. The PopPK analysis was performed with outliers omitted. Missing covariates were imputed if missing for ≤15% of the patients included in the analysis.

Modeling approach

The PopPK analysis was performed using the nonlinear mixed-effects modeling approach with the first-order conditional estimation with interaction method in NONMEM. Model parameter estimation and evaluation were implemented with NONMEM 7, Version 7.4.3 (ICON Development Solutions, Ellicott City, MD) with GNU Fortran 95 Compiler (Version 4.6), Perl-Speaks-NONMEM Version 4.2 (Uppsala University, Sweden), and R 3.5.3 (R Foundation for Statistical Computing, Vienna, Austria).

Serum tislelizumab concentrations versus time profiles were evaluated to compare the PK results across studies and doses, and to identify potential outliers for exclusion. These graphical analyses and prior knowledge of tislelizumab PK[16,17] provided initial direction for the structural model selection.

Base model and random-effects model development

Based on the known PK properties of tislelizumab,[16,17] the default structural model is a three-compartment model with first-order elimination, as illustrated in Figure 1. Alternative model structures (e.g., one-compartment, two-compartment, and three-compartment models with time-varying CL) were also explored, as appropriate. The PopPK model was parameterized in terms of CL from the central compartment, volume of the central compartment (V_c), CL of distribution from the central to the peripheral compartments (Q_2 and Q_3), and volume of the peripheral compartments (V_2 and V_3). The final base model was chosen based on the objective function value (OFV), goodness-of-fit (GOF) plots, and reliability of model parameter estimates.

Assuming a log-normal distribution, the interindividual variability (IIV) on PK parameters was described by an exponential model (Equation 1):

$$\theta_i = \exp\left(\theta_T + \eta_i\right). \quad (1)$$

θ_i = individual parameter value for the i^{th} patient, θ_T = natural logarithm of the typical value of the parameter in the population, and η_i = interindividual random effect with a mean of 0 and variance of ω^2.

Residual error was described using a combined additive and proportional error model (Equation 2):

$$C(t)_{ij} = \hat{C}(t)_{ij} \times \left(1 + \varepsilon_{pij}\right) + \varepsilon_{aij}. \quad (2)$$

$C(t)_{ij} = j^{th}$ observed serum concentration of individual i, $\hat{C}(t)_{ij} = j^{th}$ model-predicted value (serum concentration) for individual i, and $\varepsilon_{pij}/\varepsilon_{aij}$ = normally distributed residual random errors with a mean of 0 and variances of $\sigma 1^2$ and $\sigma 2^2$, respectively.

Covariate model development

Following base model development, covariates likely to impact tislelizumab PK were explored for a possible correlation with key tislelizumab post hoc PK parameters. The covariates of interest tested for inclusion in the PopPK model were baseline WT, age, sex, race, estimated glomerular filtration rate (eGFR), alanine aminotransferase (ALT), aspartate aminotransferase (AST), total bilirubin (TBIL), albumin, lactate dehydrogenase (LDH), baseline Eastern Cooperative

TABLE 1 Summary of the studies included in the tislelizumab PopPK analysis

Region	Study number	NCT number	Study description	Phase	Tislelizumab dose regimen	Patients included in PopPK model	PK samples included in PopPK model
Global	BGB-A317-001	NCT02407990	An open-label, multiple-dose, dose-escalation and -expansion study to investigate the safety, PK, and antitumor activities of the anti–PD-1 monoclonal antibody tislelizumab (BGB-A317) in patients with advanced tumors	Ia/Ib	Phase Ia: 0.5, 2, 5, or 10 mg/kg i.v. q2w; 2 or 5 mg/kg i.v. q2w or q3w; or 200 mg i.v. q3w Phase Ib: 5 mg/kg i.v. q3w[a]	450	3921
China	BGB-A317-102	NCT04068519	A study investigating safety, tolerability, PK, and preliminary antitumor activities of anti–PD-1 monoclonal antibody tislelizumab (BGB-A317) in Chinese patients with advanced solid tumors	I/II	200 mg i.v. q3w	300	2792
China	BGB-A317-203	NCT03209973	A single-arm, multicenter, phase II study of tislelizumab (BGB-A317) as monotherapy in relapsed or refractory classical Hodgkin lymphoma	II	200 mg i.v. q3w	70	346
China/Korea	BGB-A317-204	NCT04004221	A single-arm, multicenter phase II study of tislelizumab (BGB-A317) in patients with previously treated PD-L1+ locally advanced or metastatic urothelial bladder cancer	II	200 mg i.v. q3w	112	425
China	BGB-A317-205	NCT03469557	A multicohort study to investigate the safety, PK, and preliminary antitumor activity of the anti–PD-1 monoclonal antibody tislelizumab (BGB-A317) in combination with chemotherapy as first-line treatment in adults with inoperable, locally advanced, or metastatic esophageal, gastric, or gastroesophageal junction carcinoma	II	200 mg i.v. q3w	30	121
China	BGB-A317-206	NCT03432598	An open-label, multicohort study to investigate the preliminary antitumor activity, safety, and PK of the anti–PD-1 monoclonal antibody tislelizumab (BGB-A317) in combination with chemotherapy as first-line treatment in Chinese subjects with locally advanced or metastatic lung cancer	II	200 mg i.v. q3w	54	263
Global	BGB-A317-208	NCT03419897	An open-label, multicenter study to investigate the efficacy, safety, and PK of the anti–PD-1 monoclonal antibody tislelizumab (BGB-A317) in patients with previously treated hepatocellular unresectable carcinoma	II	200 mg i.v. q3w	248	974

TABLE 1 (Continued)

Region	Study number	NCT number	Study description	Phase	Tislelizumab dose regimen	Patients included in PopPK model	PK samples included in PopPK model
China	BGB-A317-209	NCT03736889	A single-arm, multicenter, open-label study to evaluate the efficacy and safety of tislelizumab (BGB-A317), an anti–PD-1 monoclonal antibody, as monotherapy in patients with previously treated locally advanced unresectable or metastatic microsatellite instability–high (MSI-H) or mismatch repair deficient (dMMR) solid tumors	II	200 mg i.v. q3w	76	288
Global	BGB-A317-302	NCT03430843	A randomized, controlled, open-label, global study comparing the efficacy of the anti–PD-1 antibody tislelizumab (BGB-A317) versus chemotherapy as second-line treatment in patients with advanced unresectable/metastatic esophageal squamous cell carcinoma	III	200 mg i.v. q3w	264	958
Global	BGB-A317-303	NCT03358875	An open-label, multicenter, randomized study to investigate the efficacy and safety of anti–PD-1 antibody tislelizumab (BGB-A317) compared with docetaxel in patients with non-small cell lung cancer who have progressed on a prior platinum-containing regimen	III	200 mg i.v. q3w	532	2271
China	BGB-A317-304	NCT03663205	An open-label, first-line therapy study of tislelizumab with chemotherapy versus chemotherapy in untreated advanced nonsquamous non-small cell lung cancer	III	200 mg i.v. q3w	222	1036
China	BGB-A317-307	NCT03594747	A multicenter, randomized, open-label study to compare the efficacy and safety of tislelizumab (BGB A317, anti–PD1 antibody) combined with paclitaxel plus carboplatin or nab paclitaxel plus carboplatin versus paclitaxel plus carboplatin alone as first-line treatment for untreated advanced squamous non-small cell lung cancer	III	200 mg i.v. q3w	238	1078
Total							
Global studies: 4 China studies: 7 Asia study: 1	N/A	N/A	N/A	Ia to III		2596	14,473

Abbreviations: i.v., intravenous; N/A, not applicable; NCT, National Clinical Trial; PD-1, programmed cell death protein 1; PD-L1, programmed death-ligand 1; PK, pharmacokinetic; PopPK, population pharmacokinetic; q2w, every 2 weeks; q3w, every 3 weeks.

[a]In Study BGB-A317-001, during phase Ia (Part 1), 22 patients received one of four escalating doses of tislelizumab q2w: 0.5 mg/kg ($n = 3$), 2 mg/kg ($n = 6$), 5 mg/kg ($n = 6$), and 10 mg/kg ($n = 7$). In Part 2, 81 patients received tislelizumab 2 mg/kg q2w ($n = 20$), 5 mg/kg q2w ($n = 20$), 2 mg/kg q3w ($n = 21$), and 5 mg/kg q3w ($n = 20$). In Part 3, 13 patients were treated with fixed-dose tislelizumab at 200 mg q3w. All patients enrolled in phase Ib of the study ($n = 335$) were treated with tislelizumab 5 mg/kg q3w.

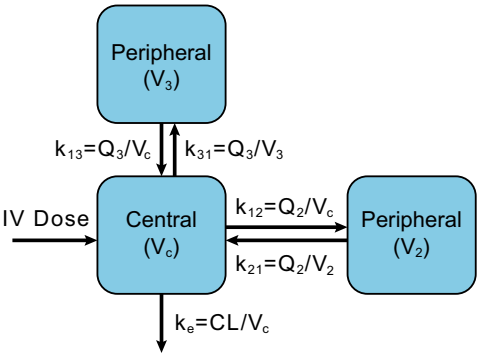

k_e=elimination rate constant
k_{12}=rate constant from central to peripheral 2
k_{21}=rate constant from peripheral 2 to central
k_{13}=rate constant from central to peripheral 3
k_{31}=rate constant from peripheral 3 to central
CL=clearance
Q_2=inter-compartmental clearance 2
Q_3=inter-compartmental clearance 3
V_c=central volume
V_2=peripheral volume 2
V_3=peripheral volume 3
IV=intravenous

FIGURE 1 Population pharmacokinetic model diagram for tislelizumab

The system is described by the following differential equations:

$$\frac{dA_c}{dt} = k_{21}A_2 + k_{31}A_3 - (k_e + k_{12} + +k_{13})A_c$$
$$\frac{dA_2}{dt} = k_{12}A_c - k_{21}A_2$$
$$\frac{dA_3}{dt} = k_{13}A_c - k_{31}A_3$$

A_c=amount of drug in the central compartment
A_2=amount of drug in the peripheral compartment 2
A_3=amount of drug in the peripheral compartment 3
t=time

Oncology Group performance status (ECOG PS; 0 vs. ≥1), ADA status (negative vs. positive), tumor size at baseline ([TUMSZ] for solid tumors; sum of products of perpendicular diameters for cHL), and tumor type (TUMTP; gastric cancer [GC], cHL, other). Baseline categorical and continuous covariates in the total population are summarized in Table 2 and presented by study in Tables S1 and S2.

The covariate effects of WT on PK parameters were tested as part of the base model development, whereas other covariates were tested after WT effects were incorporated in the base model. Once the base model was developed, covariate screening was conducted by examining the correlations between the other covariates and relevant PK parameters graphically, followed by linear regression (for continuous covariates) and analysis of variance testing (for categorical covariates) using R Version 3.5.3. These analyses were conducted using the individual empirical Bayesian estimates (EBEs) of interindividual random effects of PK parameters (η values) obtained from the final base model. Only those covariates that showed a significant ($p < 0.05$) correlation with the relevant PK parameters that could be meaningfully explained from both clinical and scientific perspectives were examined further in covariate modeling using NONMEM. Covariates were selected using a stepwise forward addition and backward elimination method based on a significance level of $p < 0.01$ for the forward steps and $p < 0.001$ for the backward steps.

Model evaluation

After completion of model development, robustness of the final PopPK model was evaluated with multiple qualification/validation methods, including diagnostic GOF plots, prediction-corrected visual predictive check (pcVPC),[18] numerical predictive check (NPC),[19] nonparametric bootstrap,[20,21] and shrinkage assessments.[22]

Covariate sensitivity analysis

The covariate sensitivity analysis was performed for the final PopPK model to examine the influence of statistically significant covariates on the predicted exposure of tislelizumab, including the area under the concentration-time curve at steady state (AUC_{ss}), the maximum concentration at steady state ($C_{max,ss}$), and the minimum concentration at steady state ($C_{min,ss}$) after the target dose of 200 mg q3w for 30 weeks. Tornado plots were generated for different scenarios (10^{th} and 90^{th} values of continuous covariates or possible group of categorical covariates) to show the influence of each covariate on expected exposure compared with the reference value, which was set as the predicted exposure in a typical male patient with tumors except cHL and GC aged 60 years, WT of 65 kg, albumin of 41 g/L, baseline tumor size of 63 mm, and ADA negative after the target dose.

PopPK model simulations

To predict the exposure of tislelizumab in the target patient population, the tislelizumab concentration-time profiles were simulated using the EBEs of individual PK parameters based on the final PopPK model for all patients following treatment with tislelizumab 200 mg q3w for 30 weeks. The predicted steady-state exposure metrics (AUC_{ss}, $C_{max,ss}$, and $C_{min,ss}$) were compared among covariate subgroups to evaluate the need for dose adjustment in patient subgroups

TABLE 2 Baseline covariates in the PopPK model development dataset

Categorical covariates	Total, $N = 2596$
Sex	
Male	1920 (74.0)
Female	676 (26.0)
Race	
White	528 (20.3)
Asian	1991 (76.7)
Black/African American	10 (0.4)
Other	44 (1.7)
Missing	23 (0.9)
ECOG PS	
0	819 (31.5)
1	1777 (68.5)
ADA	
Negative	2136 (82.3)
Positive	432 (16.6)
Missing	28 (1.1)
Therapy	
Monotherapy	2042 (78.7)
Combination	544 (21.0)
Missing	10 (0.4)
TUMTP	
cHL	70 (2.7)
CRC	81 (3.1)
EC	373 (14.4)
GC	102 (3.9)
HCC	316 (12.2)
NPC	21 (0.8)
NSCLC	1151 (44.3)
OC	52 (2.0)
UC	151 (5.8)
Other	279 (10.7)
Line(s) of therapy	
0	88 (3.4)
1	735 (28.3)
2	1076 (41.4)
3	185 (7.1)
≥4	49 (1.9)
Missing	423 (16.3)
Continuous covariates	**Total, $N = 2596$**
Age, years	60.0 (18.0, 90.0)
Weight, kg	65.0 (31.9, 130)
Albumin, g/L	41.0 (17.0, 61.3)
ALT, U/L	18.0 (2.50, 340)
AST, U/L	22.0 (5.00, 338)
Bilirubin, μmol/L	9.30 (0.513, 96.0)
eGFR, ml/min/1.73 m^2	94.9 (30.0, 162)
Creatinine, μmol/L	70.0 (21.5, 194)
LDH, U/L	207 (87.0, 6010)
TUMSZ, mm	63.3 (10, 408)

Note: Data are shown as n (%) for categorical covariates or median (minimum, maximum) for continuous covariates.

Abbreviations: ADA, antidrug antibodies; ALT, alanine aminotransferase; AST, aspartate aminotransferase; cHL, classical Hodgkin lymphoma; CRC, colorectal cancer; EC, esophageal carcinoma; ECOG PS, Eastern Cooperative Oncology Group performance status; eGFR, estimated glomerular filtration rate; GC, gastric cancer; HCC, hepatocellular carcinoma; LDH, lactate dehydrogenase; NPC, nasopharyngeal carcinoma; NSCLC, non-small cell lung cancer; OC, ovarian cancer; PopPK, population pharmacokinetic; TUMSZ, tumor size; TUMTP, tumor type; UC, urothelial bladder cancer.

of interest, including age group (<65 years, 65–75 years [≥65 and <75], ≥75 years), WT quartiles, sex, race (White, Asian, other), treatment-emergent ADAs (negative vs. positive), renal function categories (creatinine CL ≥90, 60–89, 30–59, 15–29, and <15 ml/min), hepatic function classified by National Cancer Institute Organ Dysfunction Working Group criteria (normal, mild, moderate, severe), line of therapy (first, second, third, and fourth or greater), therapy (monotherapy, combination), and TUMTP (NSCLC, esophageal carcinoma, HCC, UC, GC, colorectal cancer, cHL, ovarian cancer, nasopharyngeal carcinoma, other). To evaluate the effect of WT distribution on WT-based versus flat dosing regimens, simulations were also performed for all patients following a 3 mg/kg q3w dose regimen.

RESULTS

Base model development

Of the model structures tested, a three-compartment model with first-order elimination from the central compartment and redistribution into the peripheral compartments best characterized tislelizumab PK following i.v. administration. An Ω matrix with IIV on CL, V_c, V_2, and V_3 and covariance between CL and V_c was selected based on the model fitness as well as ETA correlation results. A combined additive and proportional error model was selected based on model fitness.

An empirical model of time-varying CL was investigated during the base model development. The relationship was modeled as follows (Equations 3 and 4):

$$CL_i = CL_T \times \exp\left(E_{time,i}\right) \times \exp\left(\eta_{CL,i}\right) \quad (3)$$

$$E_{\text{time}} = \left(T_{\max,i} + \eta_{T\max}\right) \times \frac{\text{Time}_i^r}{T_{50}^{\gamma} + \text{Time}_i^r}. \quad (4)$$

CL_i = clearance for the i^{th} patient, CL_T = typical value of clearance in the population, $\eta_{CL,i}$ = random interindividual effect for clearance, E_{time} = time-varying clearance, T_{tmax} = log maximum magnitude change in clearance, $\eta_{T\max}$ = random interindividual effect for $T_{\max}$, T_{50} = time when half $T_{\max}$ is achieved, and γ = sigmoid factor of time-varying clearance.

The results indicated that a time-varying sigmoid maximum effect ($E_{\max}$)-type model of CL did not improve the model fit.

After the base model structure was established, the model was rerun excluding 18 outlier data points with |CWRES| >5 (nine of these outliers were from Study BGB-A317-001 [2 mg/kg, $n = 3$; 5 mg/kg, $n = 6$]). Subsequently, given the previously known effect of WT on the CL and volumes of other antibodies and tislelizumab, the effects of baseline WT on CL, V_c, V_2, and V_3 were examined. The results indicated that adding the WT effect on all four parameters significantly improved the model fit ($p < 0.01$; OFV decreased by 497). However, removing the WT effect from V_2 and V_3 resulted in a nonsignificant change in OFV ($p = 0.876$; increased by 0.264). Comparison of the IIV estimates between the base model and the corresponding model without the WT effects indicated that inclusion of WT as a covariate reduced the IIV (coefficient of variation [CV]) by 12.9% and 20.8% for CL and V_c, respectively.

Covariate model development

Based on an examination of PK parameter–covariate relationships, the following had a statistical significance of $p < 0.01$ and were therefore included in the forward covariate search in NONMEM: baseline age, sex, race, eGFR, albumin, AST, LDH, ECOG PS, ADA status, tumor size, and TUMTP on CL, and age, sex, and race on V_c.

Testing of the covariates one at a time using a stepwise forward addition method in NONMEM showed that the effect of albumin, tumor size, ADAs, TUMTP, and ECOG PS on CL, and sex and age on V_c were significant ($p < 0.01$). The full PopPK model included all significant covariate relationships. ECOG PS was removed in the backward elimination process.

Final PopPK model

The original dataset included 14,786 measurable serum samples from 2601 subjects. Of these data points, 2% (313/14,786) were excluded from the PK analysis. As a result, the final PopPK analysis dataset comprised 14,473 observed serum concentrations from 2596 patients enrolled in 12 clinical studies of tislelizumab in cancer patients. A three-compartment model with first-order elimination from the central compartment and redistribution into the peripheral compartments best characterized tislelizumab PK following i.v. administration (Figure 1).

In the final PopPK model, baseline WT, age, sex, albumin, tumor size, TUMTP, and ADAs were identified as covariates with a statistically significant effect on the PK of tislelizumab, and the estimated covariate coefficients were well estimated (relative standard error ranging from 5.50% to 51.7%). The NONMEM code for the final PopPK model and output file are shown in the Supplementary Materials.

The final PopPK model included the following parameter–covariate relations (Equations 5 and 6):

$$\begin{aligned} CL_i(L/\text{hr}) = \exp\Bigg(& -5.05 + 0.565 \times \log\left(\frac{WT_i}{65}\right) - 0.457 \\ & \times \log\left(\frac{ALB_i}{41}\right) + 0.0735 \times \log\left(\frac{TUMSZ_i}{63}\right) + 0.111 \\ & \times \left(ADA_i = \text{Positive}\right) + 0.069 \times \left(TUMTP_i = GC\right) \\ & - 0.216 \times \left(TUMTP_i = cHL\right) + \eta_{CL,i} \Bigg) \end{aligned} \quad (5)$$

$$\begin{aligned} Vc_i(L) = & \exp(1.11 + 0.397) \times \log\left(\frac{WT_i}{65}\right) - 0.116 \\ & \times \left(SEX_i = \text{Female}\right) + 0.0966 \times \log\left(\frac{Age_i}{60}\right) + \eta_{Vc,i}. \end{aligned} \quad (6)$$

CL_i = clearance from the central compartment for the i^{th} individual, Vc_i = volume of distribution of the central compartment for the i^{th} individual, $\eta_{CL,i}$ and η_{Vc} = the interindividual random effects of clearance and V_c of the i^{th} individual, WT_i = body weight of the i^{th} individual, ALB_i = albumin of the i^{th} individual, $TUMSZ_i$ = tumor size of the i^{th} individual, Age_i = age of the i^{th} individual, SEX_i = sex of the i^{th} individual, and $TUMTP_i$ = tumor type of the i^{th} individual.

For a typical male patient (as described previously), the estimated CL was 0.15 L/day, V_c was 3.05 L, Q_2 was 0.74 L/day, V_2 was 1.27 L, Q_3 was 0.09 L/day, and V_3 was 2.10 L. IIVs of CL, V_c, V_2, and V_3 were 26.3%, 16.7%, 74.7%, and 99.9%, respectively.

A summary of covariate effects (evaluated for the 10th and 90th percentiles of covariate distributions) on tislelizumab PK parameters (CL and V_c) are presented in Table S3. The steady-state volume of distribution was 6.42 L, and the geometric mean elimination half-life was 23.8 days with a CV of 31%. The time to reach 90% steady-state level was approximately 84 days (12 weeks).

The general GOF plots of the final PopPK model demonstrated good agreement between the predicted concentrations and the observed concentrations, and

no apparent bias was observed in the residual plots over time and across predicted concentrations (Figures S1 and S2). Specifically, there was no trend between individual weighted residuals versus time up to approximately 3 years posttreatment (Figure S2), which indicated that the final model could describe the longitudinal observations well without the time-varying CL component. The distribution of IIV was centered at zero and was normally distributed for all parameters (Figure S3). Pairwise correlations between the ηs showed a slight correlation between CL and V_c, which is consistent with the Ω matrix structure of the model (Figure S4).

The pcVPC plots (Figure 2, Figures S5, S6, and S7) showed that the final PopPK model could adequately reproduce the central tendency and variability of the tislelizumab serum concentrations across different regimens, studies, and tumor types. The η-shrinkage for CL and V_c was low (15.9% and 15.7%, respectively), suggesting that their EBEs could be used to describe the relationships between CL or V_c and the relevant covariates (Table 3). The NPC showed that the percentage of observed data points outside the 90% prediction interval was 6.51%, suggesting that the final model adequately reproduced the distribution of the observed tislelizumab concentration data.

Covariate sensitivity analysis

The covariate sensitivity analysis showed that WT was the most influential covariate on tislelizumab exposure (Figure 3). Compared with a typical patient with a WT of 65 kg, patients with WT at the 10th and 90th percentiles of the overall population were expected to have 13.8%–18.6% higher and 11.4%–15.0% lower steady-state exposures (AUC_{ss}, $C_{max,ss}$, and $C_{min,ss}$), respectively. TUMTP had a modest effect on tislelizumab exposure: the steady-state exposures in cHL patients were up to 31.4% higher, and exposures in GC patients were 8.82% lower. The effects of albumin, tumor size, ADA status, age, and sex on tislelizumab exposure were relatively small (3.27%–10.8% for albumin, 2.81%–10.1% for tumor size, 5.39%–13.9% for ADAs, 0%–1.48% for age, and 0%–6.49% for sex). Overall, the differences in exposure due to these significant covariates were within the overall variability of exposure in the cancer patient population, which was −38.1% to +55.8%, −28.9% to 47.3%, and −48.9% to 70.8% for the 5th to 95th percentiles relative to the typical values of AUC_{ss}, $C_{max,ss}$, and $C_{min,ss}$, respectively. Other covariates evaluated (in the covariate model development and/or post hoc covariate analysis), including race, LDH, eGFR, renal function categories, hepatic function measures (AST, ALT, and TBIL) and categories, ECOG PS, therapy (monotherapy vs. combination therapy), and line of therapy did not show a statistically significant impact on the PK of tislelizumab.

PopPK model simulations

Simulations were performed to compare tislelizumab exposure with the 200 mg q3w flat dose regimen and a hypothetical 3 mg/kg q3w WT-based dose regimen to understand the effect of WT. The dose of 3 mg/kg was chosen for this

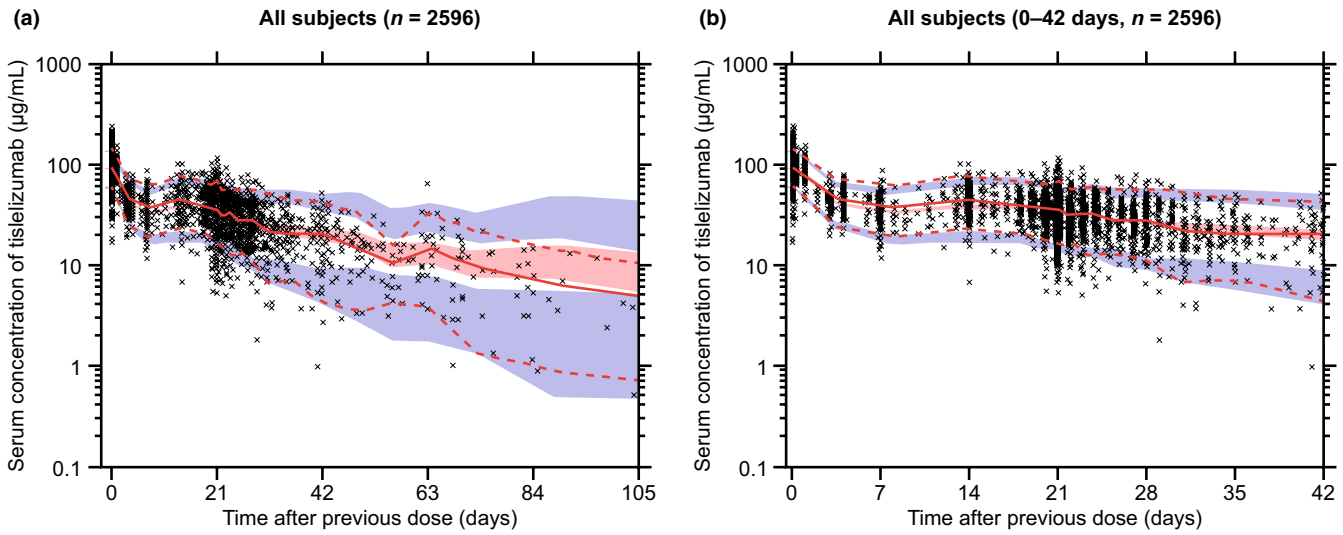

FIGURE 2 Prediction-corrected visual predictive check of tislelizumab serum concentration–time profiles across all studies in all patients from (a) 0–105 days and (b) 0–42 days. Black cross symbols are individual observed concentrations, solid red lines represent the median observed concentrations, and dashed red lines represent the 2.5th and 97.5th percentiles of the observed concentrations over time. Red shaded areas represent the 95% confidence interval (CI) of the predicted median concentrations, and the blue/purple shaded areas represent the 95% CI of the predicted 2.5th and 97.5th percentiles of the concentrations over time.

TABLE 3 Summary of final PopPK parameters

Parameter	Parameter description	Estimate (% RSE)	Median (95% CI) from bootstrapping	Shrinkage (%)
$exp(\theta_1)*24$	CL (L/day)	0.153 (0.816)	0.154 (0.151, 0.157)	15.9
θ_7	Influence of WT on CL	0.565 (5.95)	0.562 (0.491, 0.631)	–
θ_{10}	Influence of ALB on CL	−0.457 (11.2)	−0.443 (−0.648, −0.229)	–
θ_{11}	Influence of TUMSZ on CL	0.0735 (10.4)	0.0757 (0.056, 0.0953)	–
θ_{13}	Influence of ADA on CL	0.111 (13.8)	0.110 (0.0783, 0.146)	-
θ_{14}	Influence of TUMTP of GC on CL	0.069 (48.2)	0.0778 (−0.00319, 0.161)	-
θ_{15}	Influence of TUMTP of cHL on CL	−0.216 (17.1)	−0.215 (−0.294, −0.137)	-
$exp(\theta_2)$	Central volume, V_c (L)	3.05 (0.498)	3.05 (3.02, 3.08)	15.7
θ_8	Influence of WT on V_c	0.397 (5.50)	0.395 (0.354, 0.437)	-
θ_9	Influence of sex on V_c	−0.116 (8.30)	−0.116 (−0.135, −0.0997)	-
θ_{12}	Influence of age on V_c	0.0966 (51.7)	0.0957 (0.0602, 0.132)	-
$exp(\theta_3)*24$	Intercompartmental clearance, Q_2 (L/day)	0.740 (4.55)	0.746 (0.616, 0.944)	-
$exp(\theta_4)$	Peripheral volume, V_2 (L)	1.27 (2.02)	1.27 (1.14, 1.43)	55.8
$exp(\theta_5)*24$	Intercompartmental clearance, Q_3 (L/day)	0.092 (3.23)	0.0923 (0.0796, 0.104)	-
$exp(\theta_6)$	Peripheral volume, V_3 (L)	2.10 (3.89)	2.06 (1.81, 2.30)	44.4
ω^2 CL,V_c	Covariance (CL, V_c)	0.020 (6.43)	0.0198 (0.0167, 0.0227)	-
Interindividual variability (% RSE)	CL	26.3 (1.84)	26.4 (25.2, 27.7)	-
	V_c	16.7 (2.05)	16.7 (15.8, 17.6)	-
	V_2	74.7 (1.88)	76.3 (65.0, 86.8)	-
	V_3	99.9 (4.06)	97.3 (85.7, 110)	-
σ_p	Proportional residual error (%)	12.6 (1.08)	12.6 (12.0, 13.2)	17.8
σ_a	Additive residual error (μg/ml)	2.09 (9.31)	2.06 (1.79, 2.33)	17.8

Abbreviations: ADA, antidrug antibodies; ALB, albumin; cHL, classical Hodgkin lymphoma; CI, confidence interval; CL, clearance; GC, gastric cancer; PopPK, population pharmacokinetic; Q_2 and Q_3, CL of distribution from the central to the peripheral compartments; RSE, relative standard error; TUMSZ, tumor size; TUMTP, tumor type; V_c, volume of distribution in central compartment; V_2 and V_3, volume of the peripheral compartment; WT, body weight.

comparison as it corresponds to a 200 mg dose for a 65 kg patient, which is the median WT in the analysis dataset (Table S2). The extent and variability of exposure from these dose regimens were simulated from post hoc estimates from 2596 cancer patients included in the PopPK analysis.

The flat dose of 200 mg tislelizumab showed a high degree of overlap in exposures with the hypothetical 3 mg/kg dose after a single dose and at steady state (Figure S8).

The model-predicted average concentrations after the first tislelizumab dose (C_{avg1}) with 3 mg/kg q3w and 200 mg q3w across the WT range are presented in Figure 4a, and their distributions across tumor types are presented in Figure 4b. Despite the higher predicted exposures in patients with lower WT receiving the flat dosing regimen, tislelizumab exposures across the WT range were well below the median exposure observed with tislelizumab 10 mg/kg q2w, the clinically established safe and tolerable dose.[1] Moreover, the distribution of average concentration after the first dose (C_{avg1}) and average concentration at steady state ($C_{avg,ss}$) following a tislelizumab 200 mg flat dose overlapped with the distribution with a 3 mg/kg dose (Figure 4b).

Moderate differences in the geometric mean simulated exposures were observed across TUMTP (up to 34.8% for cHL and 13.6% for GC; Table S4), WT quartiles (within ±17.5%), renal function categories (within ±18.5%), and hepatic function categories (within ±15.4%) compared with the overall population geometric mean, and between White and Asian (up to 21.1%), ADA negative and positive status (up to 20.5%), and male and female (up to 19.0%). Small differences were observed in the geometric mean simulated exposures by age (<4% for adults <65 years of age, elderly patients 65–75 years of age, and elderly patients ≥75 years of age), type of therapy (<9% for monotherapy and combination therapy), and line of therapy (<7%) relative to the overall variability of exposures.

DISCUSSION

Tislelizumab PK was confirmed as linear in the tested dose range (0.5 to 10 mg/kg and 200 mg) and can be

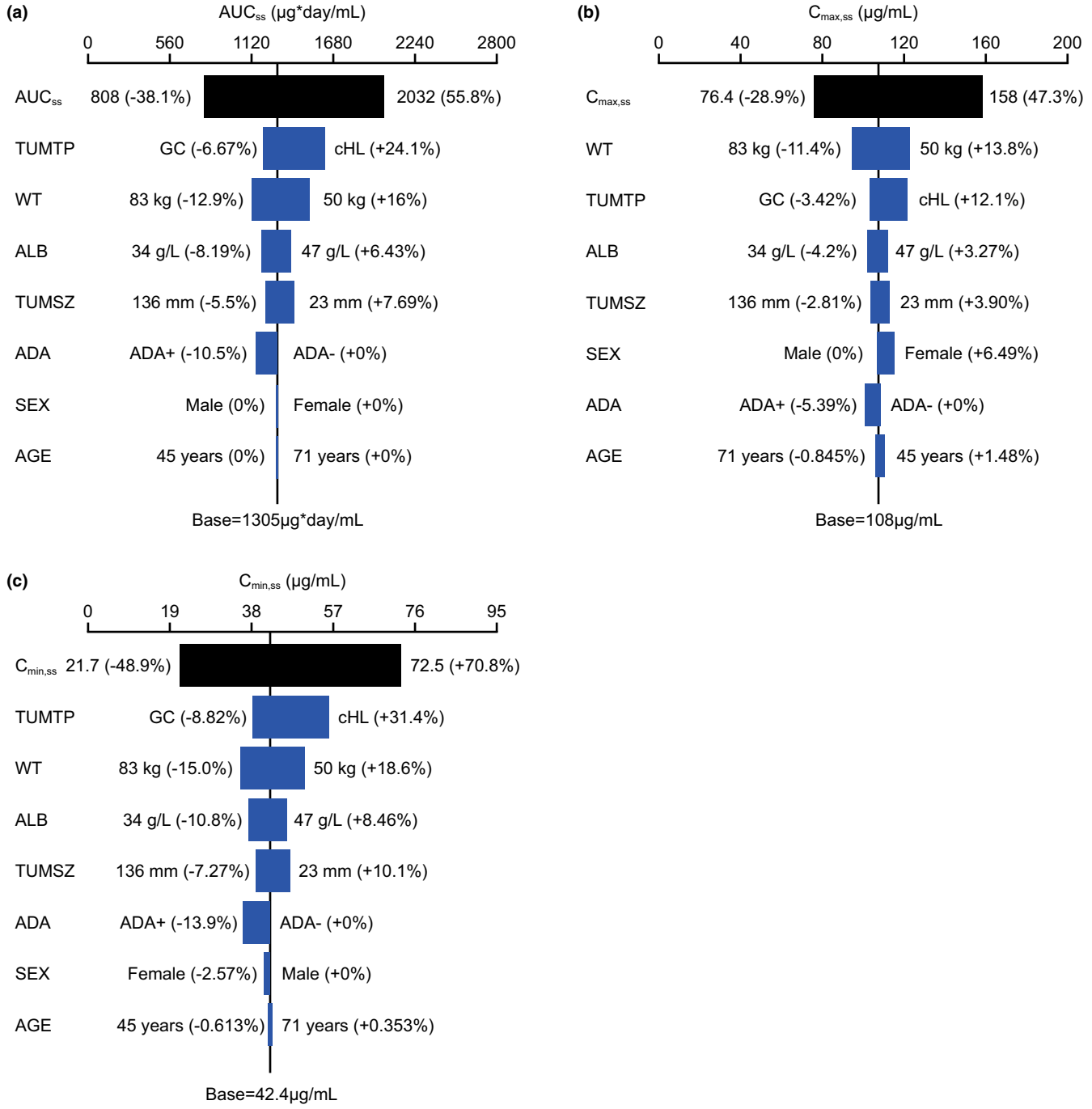

FIGURE 3 Sensitivity analysis plot comparing the effect of covariates on tislelizumab steady-state exposure for (a) AUC_{ss}, (b) $C_{max,ss}$, and (c) $C_{min,ss}$. The black vertical line refers to the predicted exposure (AUC_{ss}, $C_{max,ss}$, and $C_{min,ss}$) of tislelizumab in a typical patient after 200 mg every 3 weeks for 30 weeks (reference values). All percentage values shown in each plot are the relative changes in exposure relative to the reference value. The black shaded bar with values at each end shows the 5th to 95th percentile exposure range across the study population. Each blue shaded bar represents the magnitude of influence of the respective covariate on the exposure. The length of each bar represents the range of predicted tislelizumab exposure between the high/low or possible values of the covariate (indicated at each end of the bar). The covariates shown in each plot are ordered from the most influential covariate at the top to the least influential covariate at the bottom. ADA, antidrug antibody; ALB, albumin; AUC_{ss}, area under curve at steady state; $C_{max,ss}$, maximum concentration at steady state; $C_{min,ss}$, trough concentration at steady state; cHL, classical Hodgkin lymphoma; GC, gastric cancer; TUMSZ, tumor size; TUMTP, tumor type; WT, body weight.

adequately described by a three-compartment disposition model with linear CL. The final PopPK model well described tislelizumab PK following i.v. administration, as assessed by diagnostic GOF plots, individual fits, pcVPC, NPC, shrinkage, and nonparametric bootstrap results.

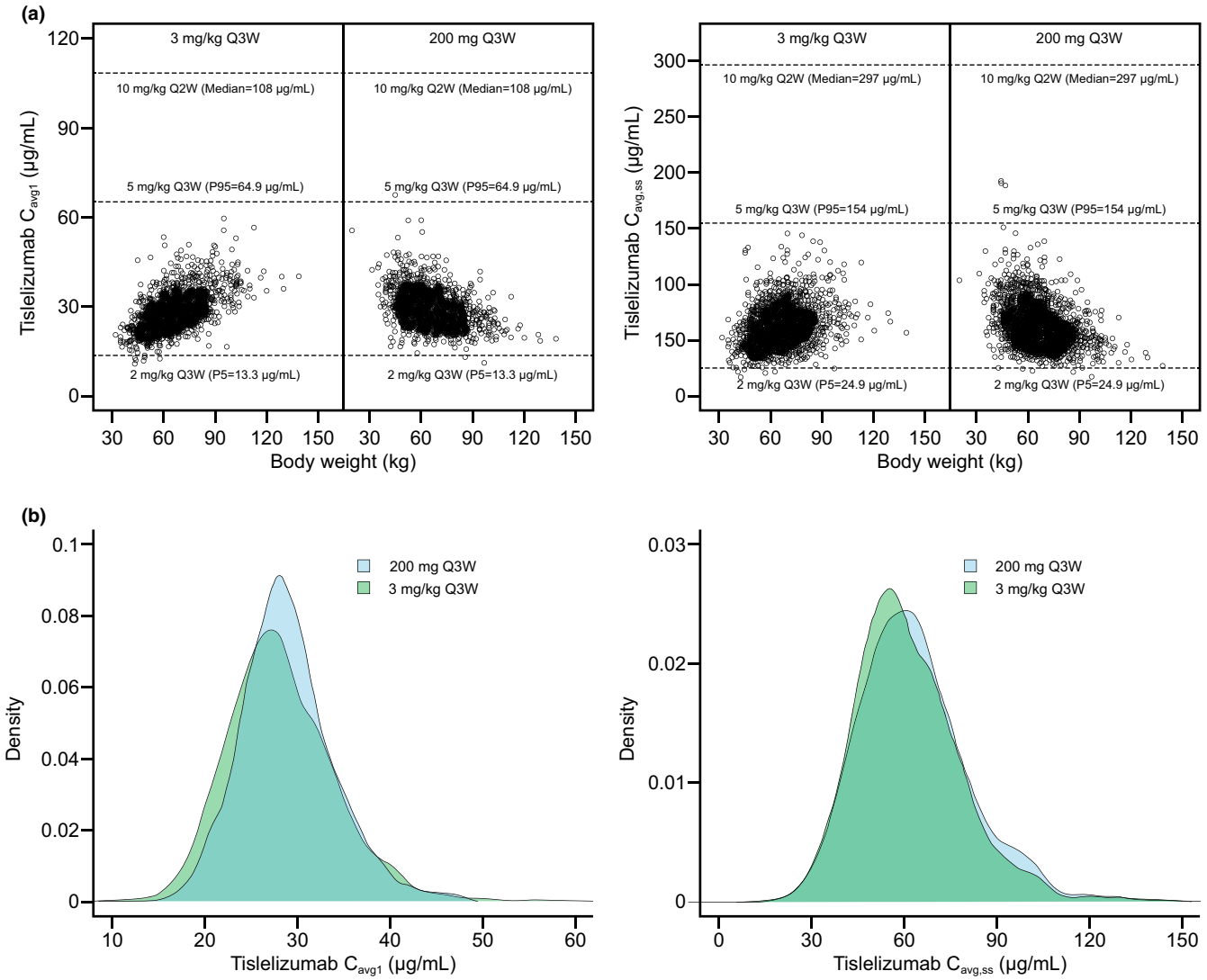

FIGURE 4 Simulated tislelizumab C_{avg1} and $C_{avg,ss}$ distribution across (a) body weight and (b) tumor types. (a) Simulated tislelizumab C_{avg1} and $C_{avg,ss}$ across body weight in patients across tumor types given 3 mg/kg q3w and 200 mg q3w (observed median body weight 65 kg from all patients). (b) Simulated tislelizumab C_{avg1} and $C_{avg,ss}$ distribution in patients across tumor types given 200 mg q3w and 3 mg/kg q3w. C_{avg1}, model-predicted average concentration after the first dose; $C_{avg,ss}$, model-predicted average concentration at steady state; P, percentile; Q2W, every 2 weeks; Q3W, every 3 weeks.

Similar to other Ig G monoclonal antibodies, tislelizumab has a low CL (0.15 L/day), limited volume of distribution (6.42 L at steady state), mainly within the extracellular fluid, and the derived elimination half-life is 23.8 days.[23] Tislelizumab had low IIV on PK parameters, which were in the typical range for monoclonal antibodies.[23] Although other marketed anti–PD-1 monoclonal antibodies, such as pembrolizumab and nivolumab, demonstrate a reduction in CL during the treatment period, as described by time-varying CL,[24,25] this phenomenon was minimal with tislelizumab based on our current pool of data from 12 clinical studies. Although there is no clear mechanistic understanding of the time-varying CL, it was hypothesized that the decrease in CL during the course of treatment may be associated with improvement in disease status.[24,25] A model allowing baseline covariates to vary over time (time-varying covariate model) provided a better fit to the atezolizumab (an anti–PD-L1 antibody) PK data than a model with empirical time-varying E_{max} CL function. These results supported the hypothesis that variation in atezolizumab CL over time is associated with a patient's disease status, as shown with other checkpoint inhibitors.[26] It was also reported that individual patient pembrolizumab CL, by incorporating the impact of on-treatment covariates (albumin, tumor size, etc.), can decrease initially and later increase during the treatment period depending on how the disease progresses, as opposed to either decrease or increase only as limited by the E_{max} model.[27] Nevertheless, it

needs to be acknowledged that time-varying CL is subject to survivorship bias, as PK samples were collected from a decreasing number of cancer patients over time and may be biased toward patients who remained in the study longer due to baseline disease characteristics, potentially better disease control, or nature of disease type with longer progression time. Therefore, variation in CL depends on a complex interplay of factors (treatment effect, course of disease, and patient characteristics). However, even for current marketed anti–PD-1/PD-L1 antibodies with observed time-varying CL, the magnitude of reduction in CL is relatively small (<25%).[25–27] Therefore, it is deemed not clinically relevant and does not warrant any clinical action in terms of dose modification.

Given the prior knowledge of the effects of WT on monoclonal antibody CL and volumes of distribution,[28] the covariate effects of WT on PK parameters were tested first and incorporated into the base PopPK model. The exponents of WT effect on CL and volume of distribution were 0.565 and 0.397, respectively. In line with most monoclonal antibodies that perform similarly between WT-based dosing and flat dosing when the exponent is <0.5 or ~0.5,[29] both regimens provided comparable PK exposures, supporting flat dosing of tislelizumab.

Baseline albumin and ADA status were identified as statistically significant covariates on CL with other disease-related covariates, including baseline tumor size and TUMTP. TUMTP had a modest effect on tislelizumab exposure: the steady-state exposures in cHL and GC patients were up to 31.4% higher and 8.82% lower, respectively, compared with those in other cancer patients. These differences are small relative to the overall variability and hence are considered clinically not relevant. The effects of albumin, tumor size, and ADA status on tislelizumab exposure were also small relative to the variability (−38.1% to 55.8%) in the whole population. Baseline tumor size was associated with increasing CL, for example, patients with smaller tumor size had 7.69% higher exposure. ADA-positive patients had 13.9% lower exposure than ADA-negative patients, likely due to the higher CL caused by the formation of ADAs. However, this difference was relatively small compared with the overall variability and was not clinically significant. Sex and age were identified as significant covariates for V_c: females had a slightly decreased V_c compared with males, and the simulated exposures in elderly subjects were up to 4% lower relative to those in adults <65 years of age. In addition, none of the hepatic or renal function–related covariates (TBIL, ALT, AST, eGFR) had significant effects on tislelizumab PK, and hence no dose adjustment is needed for patients with renal or hepatic impairment.

Overall, based on the flat exposure–response relationships observed for efficacy and safety end points (data not shown), tislelizumab exposure variations of approximately ±20% in magnitude across WT quartiles, age groups, sex, race, ADAs, renal function categories, hepatic function categories, TUMTP, therapy, and line of therapy were not deemed clinically meaningful at the dose of 200 mg q3w. This dose of tislelizumab, a regimen tested in all 12 clinical trials that formed the basis of the PopPK analysis, was selected based on the findings from study BGB-A317-001 that the PK, efficacy, and safety profiles were comparable between 2 mg/kg and 5 mg/kg dose levels, including the fixed dose of 200 mg q3w.[1] Of note, this dose is the same as that recommended for pembrolizumab in the treatment of cancers, including cHL and GC.[30] A flat exposure–response (efficacy, safety) relationship has been observed with tislelizumab. Therefore, dose adjustment of tislelizumab is not required for any special populations. Simulations of the extent and variability of exposure produced by tislelizumab showed that the PK profile of tislelizumab following flat doses of 200 mg q3w was comparable with the WT-based regimen (3 mg/kg q3w), thereby confirming that WT-based dosing does not confer additional advantages over the 200 mg q3w flat dose regimen.

CONCLUSION

PopPK modeling of tislelizumab in patients with solid tumors and hematological cancer demonstrates that tislelizumab PK is linear. The absence of covariate effects with clinical relevance supports a consistent dosing regimen for tislelizumab. Simulations with the flat dose regimen and WT-based dosing regimen showed comparable PK exposures with similar variabilities, indicating that a flat dose regimen of 200 mg q3w is appropriate in a variety of patient subpopulations.

AUTHOR CONTRIBUTIONS

N.B., C.-Y.W., Z.T., T.Y., L.L., F.X., Y.G., R.L., Q.Z., Y.W., and S.S. wrote the manuscript. N.B., C.-Y.W., Z.T., L.L., Y.G., R.L., Q.Z., Y.W., and S.S. designed the research. N.B., C.-Y.W., Z.T., F.X., R.L., Q.Z., and Y.W. performed the research. N.B., C.-Y.W., Z.T., T.Y., L.L., Y.G., R.L., Q.Z., and S.S. analyzed the data.

ACKNOWLEDGMENTS

Medical writing support, under the direction of the authors, was provided by Kirsty Millar, MSc, and Simon Lancaster, BSc, of Ashfield MedComms, an Inizio company, and was funded by BeiGene, Ltd. The

authors thank their partnered colleagues at Novartis International AG for providing their review and feedback of the manuscript.

FUNDING INFORMATION

This study was sponsored by BeiGene, Ltd.

CONFLICT OF INTEREST

N.B., C.-Y.W., Z.T., T.Y., and S.S. are employees of BeiGene (USA), Inc. L.L., F.X., and Y.G. are employees of Shanghai Qiangshi Information Technology Co., Ltd. R.L., Q.Z., and Y.W. are employees of BeiGene (Shanghai), Co., Ltd.

REFERENCES

1. Desai J, Deva S, Lee JS, et al. Phase IA/IB study of single-agent tislelizumab, an investigational anti-PD-1 antibody, in solid tumors. *J Immunother Cancer*. 2020;8:e000453.
2. Sun C, Mezzadra R, Schumacher TN. Regulation and function of the PD-L1 checkpoint. *Immunity*. 2018;48:434-452.
3. Puri S, Shafique M. Combination checkpoint inhibitors for treatment of non-small-cell lung cancer: an update on dual anti-CTLA-4 and anti-PD-1/PD-L1 therapies. *Drugs Context*. 2020;9:2019-9-2.
4. Chen S, Zhang Z, Zheng X, et al. Response efficacy of PD-1 and PD-L1 inhibitors in clinical trials: a systematic review and meta-analysis. *Front Oncol*. 2021;11:562315.
5. Chen X, Song X, Li K, Zhang T. FcγR-binding is an important functional attribute for immune checkpoint antibodies in cancer immunotherapy. *Front Immunol*. 2019;10:292.
6. Zhang T, Song X, Xu L, et al. The binding of an anti-PD-1 antibody to FcγRI has a profound impact on its biological functions. *Cancer Immunol Immunother*. 2018;67:1079-1090.
7. Feng Y, Hong Y, Sun H, et al. Abstract 2383: The molecular binding mechanism of tislelizumab, an investigational anti-PD-1 antibody, is differentiated from pembrolizumab and nivolumab. *Cancer Res*. 2019;79:2383.
8. Dahan R, Sega E, Engelhardt J, Selby M, Korman AJ, Ravetch JV. FcγRs modulate the anti-tumor activity of antibodies targeting the PD-1/PD-L1 axis. *Cancer Cell*. 2015;28:285-295.
9. Hong Y, Feng Y, Sun H, et al. Tislelizumab uniquely binds to the CC' loop of PD-1 with slow-dissociated rate and complete PD-L1 blockage. *FEBS Open Bio*. 2021;11:782-792.
10. Shen L, Guo J, Zhang Q, et al. Tislelizumab in Chinese patients with advanced solid tumors: an open-label, non-comparative, phase 1/2 study. *J Immunother Cancer*. 2020;8:e000437.
11. BeiGene Ltd. China National Medical Products Administration Approves BeiGene's Tislelizumab for Patients with Classical Hodgkin's Lymphoma Who Have Received at Least Two Prior Therapies. 2019. Accessed November 9, 2022. https://www.globenewswire.com/news-release/2019/12/28/1964740/0/en/China-National-Medical-Products-Administration-Approves-BeiGene-s-Tislelizumab-for-Patients-with-Classical-Hodgkin-s-Lymphoma-Who-Have-Received-at-Least-Two-Prior-Therapies.html
12. BeiGene Ltd. China National Medical Products Administration Approves BeiGene's Tislelizumab for Patients with Previously Treated Locally Advanced or Metastatic Urothelial Carcinoma. 2020. Accessed November 9, 2022. https://ir.beigene.com/news-details/?id=9d7cfa84-81fd-44e1-b8dc-f5d82068095a
13. BeiGene Ltd. China NMPA Approves Tislelizumab in Non-Small Cell Lung Cancer and Hepatocellular Carcinoma. 2021. Accessed November 9, 2022. https://ir.beigene.com/news-details/?id=06abb5cf-b5fa-405e-9d3b-e800e1106b99
14. BeiGene Ltd. China NMPA Approves Tislelizumab as Second- or Third-Line Treatment for Patients with Locally Advanced or Metastatic Non-Small Cell Lung Cancer. 2022. Accessed November 9, 2022. https://ir.beigene.com/news-details/?id=3e337eaa-a5f6-4368-95e0-3e0d35a71254
15. BeiGene Ltd. China National Medical Products Administration Approves Tislelizumab in Combination with Chemotherapy in First-Line Advanced Squamous Non-Small Cell Lung Cancer. 2021. Accessed November 9, 2022. https://ir.beigene.com/news-details/?id=bafd0e50-64fe-4313-9f63-a58be0fc2c54.
16. Wu CY, Tang T, Liu L, Ben Y, Sahasranaman S, Gao Y. Population pharmacokinetics of tislelizumab in patients with advanced tumors. *Ann Oncol*. 2019;30:v183.
17. Liu L, Wu CY, Wang T, Ben K, Gao Y, Sahasranaman S. Abstract 2563: Population pharmacokinetic analysis of tislelizumab in patients with advanced tumors. *Ann Oncol*. 2019;30:v159-v193.
18. Bergstrand M, Hooker AC, Wallin JE, Karlsson MO. Prediction-corrected visual predictive checks for diagnosing nonlinear mixed-effects models. *AAPS J*. 2011;13:143-151.
19. Harling K US. NPC/VPC userguide and technical description. 2013-10-16 PsN 3.6.10. 2013. Accessed November 9, 2022. https://manualzz.com/doc/36458926/npc-vpc-userguide-and-technical-description
20. Ette EI. Stability and performance of a population pharmacokinetic model. *J Clin Pharmacol*. 1997;37:486-495.
21. Karlsson M, Jonsson N, Hooker A, Harling K. *Bootstrap User Guide*. 2011. Accessed November 9, 2022. https://uupharmacometrics.github.io/PsN/docs.html
22. Savic RM, Karlsson MO. Importance of shrinkage in empirical bayes estimates for diagnostics: problems and solutions. *AAPS J*. 2009;11:558-569.
23. Dirks NL, Meibohm B. Population pharmacokinetics of therapeutic monoclonal antibodies. *Clin Pharmacokinet*. 2010;49:633-659.
24. Li H, Yu J, Liu C, et al. Time dependent pharmacokinetics of pembrolizumab in patients with solid tumor and its correlation with best overall response. *J Pharmacokinet Pharmacodyn*. 2017;44:403-414.
25. Bajaj G, Wang X, Agrawal S, Gupta M, Roy A, Feng Y. Model-based population pharmacokinetic analysis of nivolumab in patients with solid tumors. *CPT Pharmacometrics Syst Pharmacol*. 2017;6:58-66.
26. Marchand M, Zhang R, Chan P, et al. Time-dependent population PK models of single-agent atezolizumab in patients with cancer. *Cancer Chemother Pharmacol*. 2021;88:211-221.
27. Li H, Sun Y, Yu J, Liu C, Liu J, Wang Y. Semimechanistically based modeling of pembrolizumab time-varying clearance using 4 longitudinal covariates in patients with non–small cell lung cancer. *J Pharm Sci*. 2019;108:692-700.
28. Thomas VA, Balthasar JP. Understanding inter-individual variability in monoclonal antibody disposition. *Antibodies (Basel)*. 2019;8:56.
29. Bai S, Jorga K, Xin Y, et al. A guide to rational dosing of monoclonal antibodies. *Clin Pharmacokinet*. 2012;51:119-135.
30. Centanni M, Moes DJAR, Trocóniz IF, Ciccolini J, van Hasselt JGC. Clinical pharmacokinetics and pharmacodynamics

of immune checkpoint inhibitors. *Clin Pharmacokinet*. 2019;58:835-857.

SUPPORTING INFORMATION

Additional supporting information can be found online in the Supporting Information section at the end of this article.

How to cite this article: Budha N, Wu C-Y, Tang Z, et al. Model-based population pharmacokinetic analysis of tislelizumab in patients with advanced tumors. *CPT Pharmacometrics Syst Pharmacol*. 2022;00:1-15. doi: 10.1002/psp4.12880